Applied Catalysis B: Environmental 91 (2009) 481–488

Contents lists available at ScienceDirect

Applied Catalysis B: Environmental

journal homepage: www.elsevier.com/locate/apcatb

Self-cleaning modified TiO_2–cotton pretreated by UVC-light (185 nm) and RF-plasma in vacuum and also under atmospheric pressure

M.I. Mejía [a], J.M. Marín [a], G. Restrepo [a], C. Pulgarín [b], E. Mielczarski [c], J. Mielczarski [c], Y. Arroyo [d], J.-C. Lavanchy [e], J. Kiwi [b,*]

[a] Applied Physicochemical Processes Research Group, Faculty of Engineering, University of Antioquia, Street 67 53-108, AA 1226, Medellin, Colombia
[b] Institute of Chemical Sciences and Engineering, SB, GGEC Station 6, Ecole Polytechnique Fédérale de Lausanne (EPFL), 1015, Lausanne, Switzerland
[c] INPL/CNRS, UMR 2569 LEM, 15 Av du Charmois, 54501, Vandoeuvre les Nancy, France
[d] CIME EPFL, Bât MXC-134, Station 12, 1015, Lausanne, Switzerland
[e] IMG-Centre d'Analyse Minérale Bât Anthropole, Univ Lausanne, CH-1015, Lausanne, Switzerland

ARTICLE INFO

Article history:
Received 14 March 2009
Received in revised form 16 May 2009
Accepted 18 June 2009
Available online 24 June 2009

Keywords:
RF-plasma
UVC-light
Photocatalysis
Self-cleaning
Wine stains
Cotton fabrics
TiO_2

ABSTRACT

Two new innovative findings presented in this study are: (a) TiO_2–cotton fabrics obtained by pretreatment with UVC-light (185 nm) at atmospheric pressure introduced functionalities into the cotton surface enabling the chelation/binding of TiO_2. This was possible since the molar absorption coefficient of O_2 and N_2 is very low at 185 nm and (b) the radiofrequency (RF-plasma) pretreatment of cotton surface lead to the formation active binding sites on the cotton at atmospheric pressure. This unexpected RF effect was due to the drastic localized heating of the cotton leading to intermolecular H-bond breaking between the cellulose surface-OH groups of adjacent molecules with the formation of functionalized groups in the cellulose fibers. The discoloration kinetics of the wine stain on the TiO_2–cotton pretreated by RF at atmospheric pressure for 10 min was the most favorable. The red wine stains discoloration under Suntest simulated light was monitored by diffuse reflectance spectroscopy (DRS) and by the CO_2 evolution during the stain mineralization. By X-ray photoelectron spectroscopy (XPS) it was possible to monitor the decrease of the C, N, S-species on the textile topmost layers during the discoloration process. The XPS Ti $2p_{3/2}$ peak shifts indicating Ti^{4+}/Ti^{3+} oxido-reduction taking place during the photocatalysis. X-ray diffraction showed the formation of the anatase phase on the cotton. By X-ray fluorescence the loading of TiO_2 before and after the discoloration process was found to be ~0.8%. High-resolution electron microscopy (HRTEM) shows transparent TiO_2 anatase 8–18 nm coating the cotton with layers ~31 nm (±10%). These 3–4 TiO_2 layers on the cotton did not affect the touch or handling properties of the cotton enabling the potential commercial use of the TiO_2–cotton fabrics.

1. Introduction

Photocatalysts have gained in attention in the recent years because these materials enable low energy and low cost processes [1,2]. Among these photocatalysts, nanocrystalline TiO_2 is widely used in water [3–9] and air purification [9–16], in self-cleaning process [17–21] and as bactericide under light irradiation [20–28]. Photocatalysis with TiO_2 anatase is more efficient than rutile or brookite. Nanocrystalline anatase is commonly prepared with high surface area having a high degree of crystallinity [19,25].

TiO_2 coated on surfaces such as glass, fabrics, cement and plastics had been recently reported [9,10,12–25]. Recently, fabrics modified with TiO_2 have been the subject of several studies focusing on pretreatment fabric process [29–33], coating methods [34–37] and TiO_2 particles synthesis and deposition [30–32,38–44]. Also TiO_2 coated fabrics have been applied in pollutant degradation [34,37,42,45,46], self-cleaning [29–33,39–41,43,47] and bacterial inactivation [30,38,48]. Bozzi et al. have reported recently 2005 [31], the pretreatment of natural and synthetic fibers by RF-plasma, MW-plasma and vacuum-UV radiation (V-UV) leading to the formation of active sites/chelating groups species formation on the fiber surface. This facilitates the binding of the slightly positive TiO_2 on the textile surface making possible a stable self-cleaning activity [29,31,32]. Furthermore, chemical spacers to attach TiO_2 on the cotton textile surface have also been explored [33]. Qi et al. reported the pretreatment of polyester fibers by low-temperature oxygen RF-plasma and their use in self-cleaning process [30].

Cotton is a natural fiber widely used for about 7000 years [49]. World production of cotton is currently 24 million tons per annum

* Corresponding author.
E-mail address: john.kiwi@epfl.ch (J. Kiwi).

0926-3373/$ – see front matter © 2009 Elsevier B.V. All rights reserved.
doi:10.1016/j.apcatb.2009.06.017

[50], mainly in clothing, medical household fabrics, etc. RF-plasma and vacuum-UV are employed in this study for the pretreatment of cotton fabrics. Pretreatments modify the structure of cotton surface introducing a variable density of negative groups COO^{2-}, $-O-O^{2-}$, phenols, lactams and other organic anions. Then the TiO_2 binds to the modified textile through the slightly positive Ti^{4+} of the TiO_2 through electrostatic attraction/chelation with the COO^{2-}, $-O-O^{2-}$ negative groups of the textile surface. The self-cleaning performance of coated textiles was monitored through the discoloration of red wine stains under simulated solar light.

We report for the first time the discoloration of wine stains (a) on TiO_2 cotton by RF-plasma at atmospheric pressure and (b) far-UV (185 nm) or UVC radiation also at atmospheric pressure and discuss the two different mechanisms taking place. These processes are traditionally carried out in moderate vacuum atmospheres [41,51]. The findings in this study are explained and may have a wide application potential to fix nanoparticulates on the textiles surfaces avoiding the expensive vacuum associated with the traditional pretreatment methods.

2. Experimental

2.1. TiO_2 colloidal synthesis

Titanium isopropoxide (97%, Aldrich Chemical Co.) was added dropwise to 0.1 M nitric acid solution (125–750 mL respectively) under vigorous stirring. White slurry formed and this slurry was heated to 80 °C, stirred for 3 h to achieve peptization (i.e., destruction of the agglomerates and re-dispersion into primary particles). The solution was then filtered in a funnel provided with a glass frit to remove non-peptized agglomerates. Hydrothermal treatment of the solution in an autoclave was carried out for 12 h at 250 °C. Sedimentation occurs during the autoclaving, and the particles are re-dispersed by two consecutive sonications. Then the colloidal suspension is introduced in a rotary evaporator set at 35 °C, 3 MPa and brought to a final TiO_2 concentration of 11 wt%.

2.2. Functionalization of textile fibers by RF-plasma

Cotton 100% fabric was used as support material for TiO_2 particles, because of their good flexibility, large surface and good absorbing power. The cotton was mercerized and had been treated with a variety of stabilizers, oxidants and tensides to eliminate the natural grease, pectine, lignine and stains associated with untreated cotton fibers. This fabric was pretreated in a RF-plasma cavity (Harrick Corp., 13.56 MHz, power 100 W). Cotton samples were pretreated for 5, 10 and 30 min with RF-plasma, at pressures of 0.1 mbar and also without vacuum.

Generally for RF-plasma formation low pressures are needed to enhance the capture length of the electrons generated in the electric field having a higher ionization potential that the one of the gas. This condition allows the plasma discharge to occur. But without vacuum as in our experiments conducted at the low RF-plasma power of 100 W, the RF-pretreatment was only able to induce localized heating in the cotton breaking intermolecular bonds (H-bonds) and partially segmenting the textile at temperatures far above 160 °C [51]. This introduces functional groups C–O–, –OOH, –O–C=O, –COH, –COOH on cotton, in the plasma cavity and in the presence of O_2 (air), that allow the attachment of TiO_2 by exchange/impregnation as described below in Section 2.4 [52,53].

Table 1
Conditions used to load TiO_2 on cotton textiles.

Sample number	Type of pretreatment	Time of pretreatment (min)
1	RF-plasma	30
2	RF-plasma	10
3	RF-plasma	5
4	RF-plasma without vacuum	30
5	RF-plasma without vacuum	10
6	RF-plasma without vacuum	5
7	Vacuum-UV	30
8	Vacuum-UV	10
9	Vacuum-UV	5
10	UV without vacuum	30
11	UV without vacuum	10
12	UV without vacuum	5

2.3. Functionalization of textile fibers by vacuum-UV

The textile polymer surface was also functionalized by UV irradiation using the 185 nm line (6 W) from a 25 W (254 + 185 nm light) low-pressure mercury lamp (Ebara Corp., Tokyo, Japan). Samples were also prepared without vacuum. UV activation having a lower energy than the RF-plasma, does not lead to cationic or anionic oxygen species in the gas phase. Only atomic (O) and excited oxygen (O^*) species are formed since we irradiate with 185 nm light below the 241 nm (495 kJ/mol) required for the reaction $O_2 \rightarrow 2O^*$ [31,32]. The absence of cationic or anionic oxygen species lead to a more uniform TiO_2 layer of the textile surfaces as found by HRTEM and described below in Section 3.7.

For the case of the textile on the UVC cavity, the distance between the samples and the cylindrical UVC-light source was 3 mm. The O_2 cross-section is 10^{-20} cm^2 and the molar absorption coefficient εO_2 (185 nm) $\approx$2.6 M^{-1} cm^{-1}[54]. The cross-section of N_2 is about 10 times smaller than for O_2 at this wavelength. Therefore the εN_2 (185 nm) would negligible. At 185 nm the extinction coefficients of O_2 and N_2 are so low, that practically no UVC-radiation is lost in the optical pathway between the light source and the cotton sample even at atmospheric pressures.

2.4. Loading of TiO_2 on pretreated cotton fabrics

After functionalizing the textile surfaces by both pretreatments the fabrics were immersed in TiO_2 Degussa P25 colloidal solutions (3 g/L) and impregnated/exchanged for 30 min. Afterwards, the samples were dried in two steps: (a) first in air for 24 h at 22 °C (room temperature) and (b) followed by heating at 100 °C for 15 min. Samples prepared are showed in Table 1. The samples were immersed immediately after pretreatment since the functional groups introduced at the fabric surface deactivate reacting with the

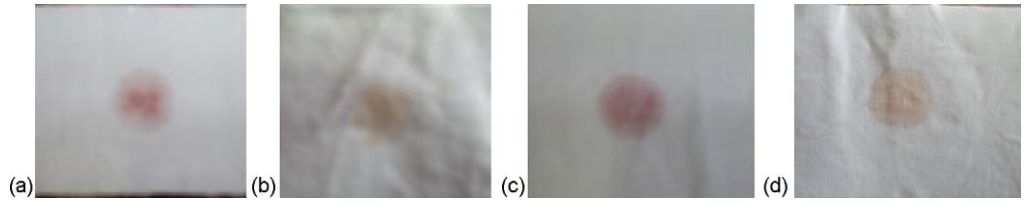

Fig. 1. Discoloration of wine stains on TiO_2–cotton: pretreated by RF for 10 min no vacuum (a) before and (b) after Suntest irradiation, pretreated by UVC for 10 min, in vacuum (c) before and (d) after Suntest irradiation.

Table 2
Surface atomic concentration in % cotton XPS results.

Sample	O	O			Ti	N	C	C			Ca	S	Si	K	P
		529 eV	53 eV	532 eV				284.6 eV	286.2 eV	288.1 eV					
Cotton ref	26.38		7.9	92.1		0.36	71.98	52.27	36.77	10.95	0.41	0.24	0.6		
Cotton + TiO_2 t = 0 h	47.56	74.03	13.81	12.16	17.18	0.42	34.84	71.22	17.55	11.23					
Cotton + TiO_2 + wine t = 0 h	26.29	4.9	5.94	89.16	0.56	1.38	71.36	54.41	40.83	4.76		0.41			
Cotton + TiO_2 + wine t = 3 h	36.37	27.14	10.5	62.36	4.69	1.06	57.24	43.61	41.05	15.34		0.15		0.16	0.34
Cotton + TiO_2 + wine t = 6 h	35.44	37.91	7.05	55.04	5.76	1.16	56.84	49.36	38.47	12.17		0.2		0.18	0.40
Cotton + TiO_2 + wine t = 24 h	46.5	57.09	9.99	32.92	10.06	1.12	41.50	43.28	35.94	20.78		0.08		0.18	0.59

humidity and oxygen of the air [31]. The samples were then washed with distilled water to remove TiO_2 particles that did not attach to the cotton surface.

2.5. Irradiation and evaluation of the textile self-cleaning action. CO_2 evolution

Cylindrical Pyrex reactors (50 mL) containing strips of TiO_2 coated textiles (9 cm^2) were positioned immediately behind the reactor wall. The red wine stains were introduced on the cotton fabric using a 70 μL micro-syringe. The irradiation of the samples was carried out in a Suntest solar simulator CPS (Atlas GmbH) equipped with a Xe-lamp (830 W). This solar cavity has a spectral distribution with 0.5% of the photons at wavelengths <300 nm, and 7% between 300 and 400 nm. The emission spectrum between 400 and 800 nm follows the solar spectrum. All the internal walls of the Suntest were of Al reflective material in order to conduct the maximum irradiation to the Pyrex vessels.

The CO_2 produced during irradiation was measured in a gas chromatograph (Carlo Erba, Milano) provided with a Poropak S column.

2.6. X-ray photoelectron spectroscopy (XPS)

XPS analyses were carried out on an X-ray photoelectron microscope Kratos model Axis Ultra. The XPS was performed using Mg K_α radiation of 150 W. The electron energy analyzer (Leybold EA200) was operated at band-pass energy of 75 eV in the pre-selected transmission mode. The binding energy of the spectrometer was referenced to 84.0 eV for the Au $4f_{7/2}$ signal according to the SCA A83 standard of the National Physics Laboratory [55]. The evaluation of the binding energies of the embedded TiO_2 was carried out following the standard procedures [56]. A reproducibility of ±5% was attained in the XPS measurements. The ADS100 set was utilized to evaluate the XPS data by subtraction of X-ray satellites applying the background correction according to Shirley [55].

2.7. Diffuse reflectance spectroscopy (DRS)

Diffuse reflectance spectra were measured using a Cary 5 UV–vis–NIR spectrophotometer equipped with an integration sphere. Measurements were carried out on 2.5 cm × 2.5 cm size samples.

2.8. X-ray diffraction measurements (XRD) of TiO_2-loaded textiles

The crystallinity and phase of the TiO_2 loaded on the textile surface was studied with a Siemens X-ray diffractometer using Cu Kα radiation.

2.9. High-resolution transmission electron microscopy (HRTEM) of TiO_2-loaded textiles

A Philips CM 300 (field emission gun, 300 kV, 0.17 nm resolution) HRTEM microscope and a Philips EM 430 (300 kV, LaB_6, 0.23 nm resolution) were used to measure the particles sizes of the titania clusters coating the textile fabrics. The textiles were embedded in epoxy resin (Embed 812) and the fabrics were cross-sectioned with an ultra-microtome (Ultracut E) to a thin section of 50–70 nm. Magnification from about 3000× to 41000× was used to characterize the samples and determinate TiO_2 cluster size.

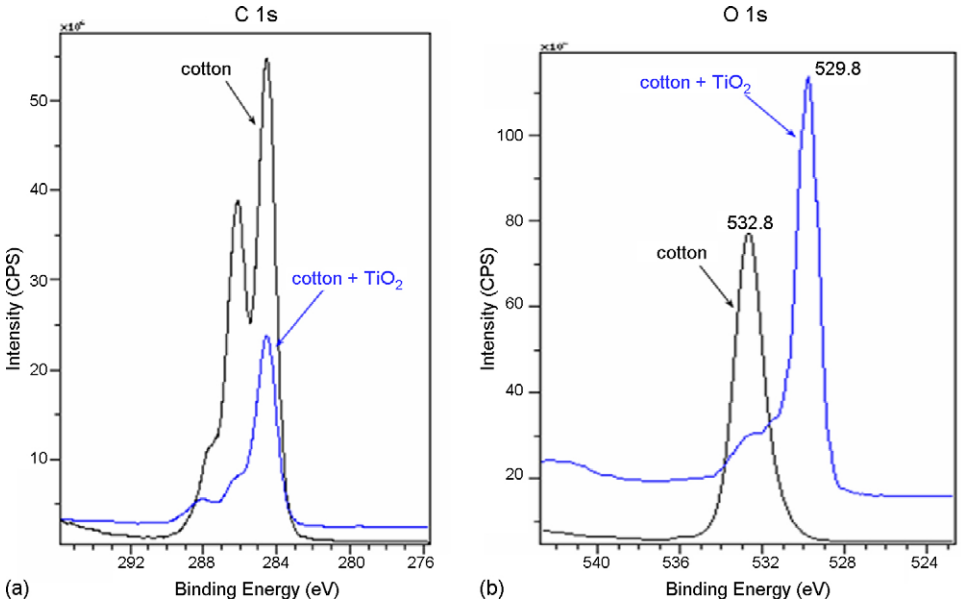

Fig. 2. XPS spectrum of cotton fabric, no pretreatment (a) C 1s peak and (b) O 1s peak.

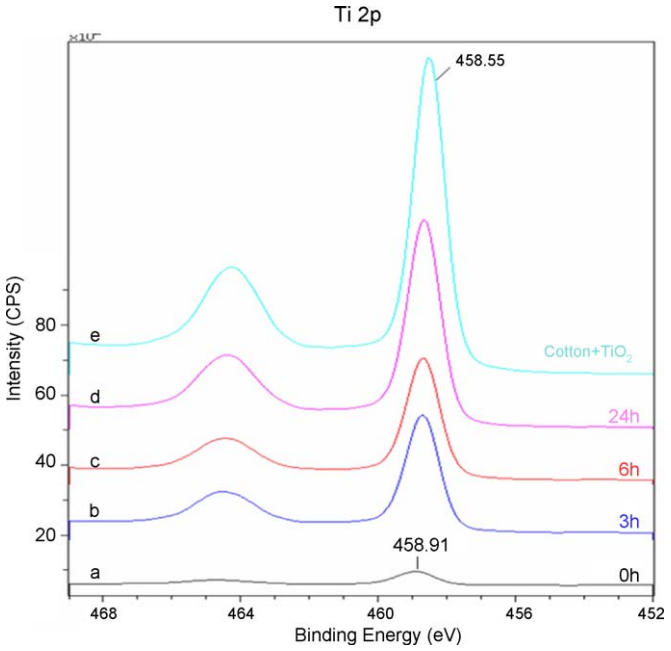

Fig. 3. XPS spectrum of Ti 2p peaks of TiO_2–cotton stained with wine pretreated for 10 min, no vacuum and irradiated with Suntest light for (a) 0 h, (b) 3 h, (c) 6 h, (d) 24 h and (e) TiO_2-coated cotton pretreated in the same way without wine at 0 h.

2.10. X-ray fluorescence determination of Ti-content on the cotton surface

The cotton TiO_2 content of loaded fabrics were evaluated by X-ray fluorescence and were determined to be ~0.8% in Ti (in experimental error of 10%) for the UVC pretreated TiO_2–cotton fabrics before and after the discoloration process and ~0.9%Ti for the RF-pretreated TiO_2–cotton fabrics. In this technique each element emits an X-ray of a certain wavelength associated with its particular atomic number. The spectrometer used was RFX, PANalytical PW2400.

3. Results and discussion

3.1. Discoloration of red wine stains on TiO_2-coated cotton fabric

Fig. 1a–d shows the wine stain on pretreated cotton by RF and UVC, respectively, before and after 24 h of Suntest irradiation. In

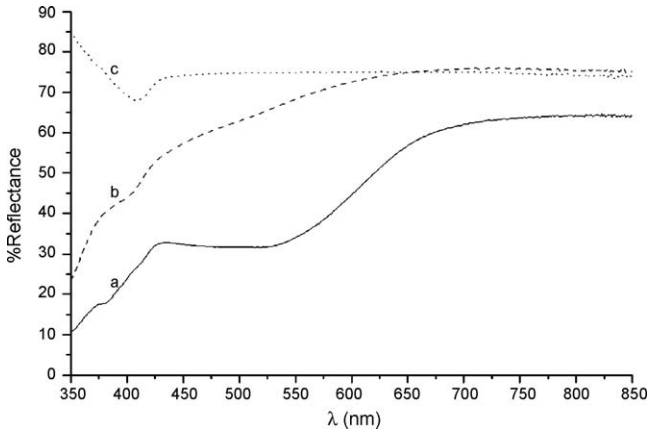

Fig. 4. Diffuse reflectance spectra of (a) TiO_2-coated cotton for 10 min, no vacuum stained with wine before irradiation, (b) same TiO_2-coated cotton sample stained with wine after 24 h Suntest irradiation and (c) cotton fabric.

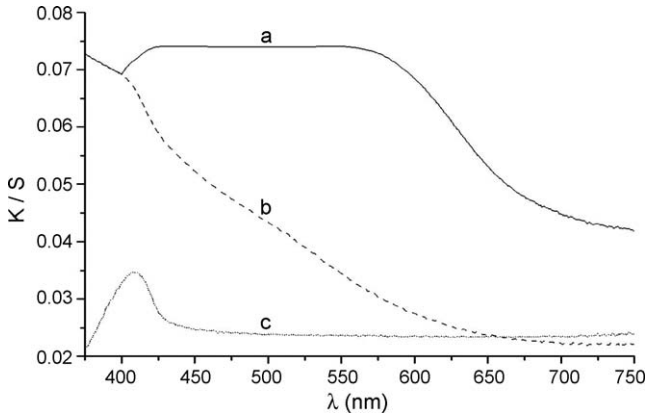

Fig. 5. Kubelka–Munk relations of (a) TiO_2-coated cotton pretreated for 10 min, no vacuum stained with wine before irradiation, (b) TiO_2-coated cotton stained with wine after 24 h Suntest irradiation and (c) cotton fabric.

both cases, partial discoloration of the wine stain was observed. It means that both pretreatment bind TiO_2 effectively on the cotton leading to discoloration within 24 h. "After drying Suntest irradiation for 24 h was conducted on the samples and the discoloration as well as the CO_2 evolution (see Section 2.5) for the pretreated by RF-plasma for 10 min, no vacuum, provided the same discoloration and released a similar amount of CO_2."

3.2. XPS of TiO_2-loaded fabric and evaluation of wine stain degradation

Table 2 shows the surface atomic concentration in % for O, Ti, C, Ca, S, Si and K of the RF-plasma pretreated coated TiO_2. Table 2 shows a value of 47.56% for the O of cotton + TiO_2 at time zero. This value decreases after wine as added at 3 and 6 h and regains the initial value after 24 h when TiO_2 is again on the cotton surface after wine discoloration. The same trend is observed for Ti. The C-content of the top surface fibers decreases with discoloration since the wine spot is discolored allowing the TiO_2 to be on the topmost layer.

Fig. 2a shows the C 1s XPS lines at 284.6, 286.2 and 287.7 eV for TiO_2–cotton samples. These peaks are due to the presence of C–C, C–O and C═O groups [57] for cotton. The O 1s line at 532.8 eV of

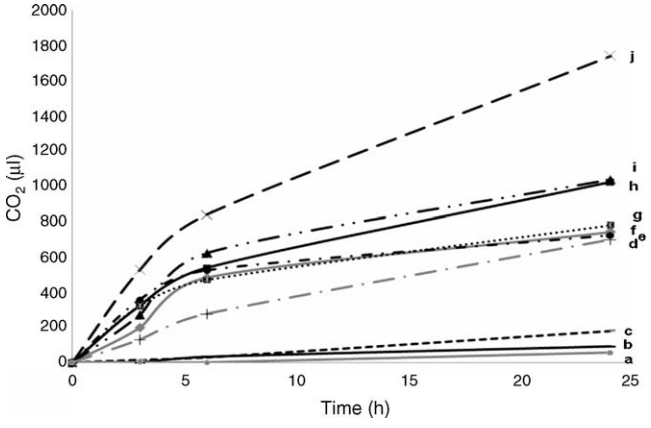

Fig. 6. CO_2 evolution under Suntest light irradiation for RF-pretreated samples of (a) cotton alone, no vacuum, pretreated for 10 min (b) cotton + wine stain, no vacuum, pretreated for 10 min (c) cotton + TiO_2 without pretreatment, atmospheric pressure (d) cotton + TiO_2 without pretreatment + wine stain, atmospheric pressure (e) cotton sample + wine stain, pretreated for 5 min in atmospheric pressure (f) cotton sample + wine stain, vacuum, pretreated for 30 min (g) cotton sample + wine stain, vacuum, pretreated for 5 min (h) cotton sample + wine stain, no vacuum, pretreated for 30 min (i) cotton sample vacuum, pretreated for 10 min + wine stain and (j) cotton sample no vacuum, pretreated for 10 min + wine stain.

this sample is shown in Fig. 2b. The reference sample of cotton shows the presence of small amounts of nitrogen, calcium, sulphur and silicon on its surface (not showed in the XPS spectrum).

After the TiO_2 coating, the TiO_2 was observed as the major product indicating a uniform distribution of the catalyst on the cotton surface. The observed signal from cotton after TiO_2 deposition (Fig. 3) indicates that TiO_2 coating predominates at the catalyst surface as a thin film about 30 nm thick. This TiO_2 layer lowers significantly the signal from cotton substrate. Regarding the O 1s in Fig. 2b after coating, a peak with a binding energy of 529.8 is observed due to for O–Ti^{4+} link [31,57,58] of a uniform TiO_2 layer covering completely the cotton surface.

Fig. 3a and b shows the XPS for samples stained with red wine as a function of the irradiation time. The drop of wine deposited on functionalized cotton significantly changes the XPS spectra. The most striking observation is that wine produces a deposit 30–40 nm that attenuates the signal of the Ti 2p peak from the wine/TiO_2 cotton sample taken at time zero (upper peak). It is noticed that Ti 2p peaks grows significantly after 3 h of oxidation reaction (Fig. 3a and b). This indicates that after 3 h exposition significant removal of wine deposit (stain) took place. After 24 h of reaction Ti signal reaches around 70% of initial intensity (Fig. 3d and e) indicating an advanced degree of destruction of the wine stain. In Fig. 2 the Ti $2p_{3/2}$ peak showed a shift from 458.91 eV at zero time to 458.65 eV after 24 h reaction. This small but significant shift indicates redox catalysis involving two oxidation states Ti^{4+}/Ti^{3+} taking place during the discoloration process.

Close inspection of other XPS lines C 1s, O 1s and S 2p supports the conclusion of wine deposit removal by oxidation reactions on the following grounds: (a) C 1s line. In Fig. 2a which indicates higher intensity ratio between the line components at 286.2 eV (C–O) and 284.6 eV (C–C) with reaction time. More oxidized carbon intermediates were observed on the textile surface with simultaneous lowering of total carbon when reaction progresses and (b) moreover S 2p line in the XPS spectrum (not shown) at zero time of reaction shows two sulfur components at around 168.0 eV characteristic of the SO_4^{2-} groups and around 163.5 eV characteristic for S^{2-} molecular group. The sulfide (S^{2-}) is oxidized to SO_4^{2-} and the sulfate was progressively removed from the catalyst surface at longer reaction times.

3.3. Diffuse reflectance spectroscopy of wine stain discoloration on TiO_2–cotton

DRS spectra of TiO_2-coated cotton pretreated by RF for 10 min, no vacuum and stained with red wine are showed in Fig. 4a, two absorptions ranges are observed. On $\lambda < 400$ nm the absorption is due to TiO_2 and a second absorption in the visible range comes from the red wine stain. After 24 h Suntest light irradiation, a sharp increase in reflectance is observed due to the red wine discoloration (Fig. 4b).

Fig. 5 shows the absorption for the DRS-reflectance reported in Fig. 4. The Kubelka–Munk relations were used to transform the reflectance into absorption data [58]. Diffuse reflectance (R))can be related to the absorbance by the K/S ratio using the Kubelka–Munk relations ($F(R)$) in (Eq. (1)). The term K is the absorbance of the sample and the reflectance relates to the absorption coefficient (K/S) [58], where S is associated with the scattering and the reflectance is noted as R.

$$\frac{K}{S} = \frac{(1 - R_\infty)^2}{2R_\infty} \equiv F(R_\infty) \quad (1)$$

Fig. 5a shows the TiO_2-cotton-red wine stain pretreated for 10 min, no vacuum before irradiation having an absorption shoulder between 425 and 590 nm due to the tannins, carotene, porphyrin and flavins pigments found in red wine [59]. Furthermore, the absorption of cotton is seen in Fig. 5c. After 24 h Suntest irradiation, a decrease in absorption of the wine stain was observed (Fig. 5b).

3.4. CO_2 evolution on the degradation of wine stain on cotton fabric

3.4.1. CO_2 evolution of cotton fabrics pretreated by RF-plasma with and without vacuum

Wine stains are mineralized under Suntest irradiation

$$C_xH_yN_zS_w + H_2O\nu + O_2(\text{air}) \rightarrow CO_2 + SO_p + NO_q + H_2O \quad (2)$$

Fig. 6 shows the evolution of CO_2 during the wine stain discoloration as a function of irradiation time on samples pretreated by RF-plasma. Samples pretreated by RF-plasma without vacuum for 10 min (Fig. 6 trace J) produce the highest

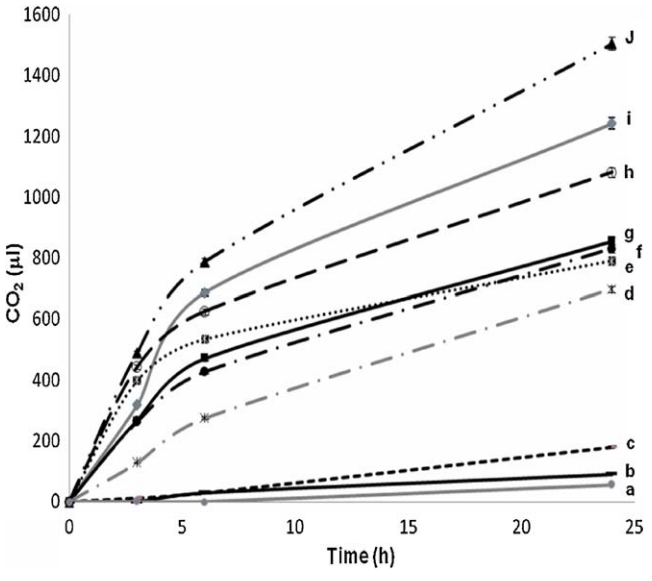

Fig. 7. CO_2 evolution under Suntest light irradiation for UVC pretreated samples of (a) cotton alone, pretreated for 10 min in vacuum (b) cotton + wine stain, pretreated for 10 min in vacuum (c) cotton + TiO_2 pretreated for 10 min in vacuum, (d) cotton + TiO_2 + wine stain, pretreated for 10 min in vacuum (e) cotton sample + wine stain, pretreated for 5 min in vacuum (f) cotton sample + wine stain, pretreated for 10 min no vacuum (g) cotton sample + wine stain, pretreated for 10 min in vacuum (h) cotton sample + wine stain, pretreated for 10 min no vacuum (i) cotton sample + wine stain, pretreated for 30 min in vacuum and (j) cotton sample + wine stain, pretreated for 10 min in vacuum.

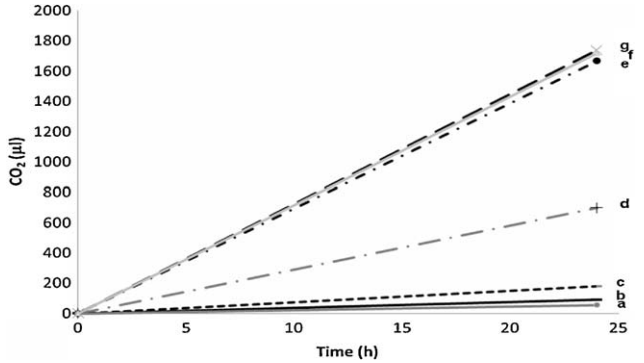

Fig. 8. CO_2 evolution under Suntest light irradiation for TiO_2–cotton samples RF-plasma pretreated for 10 min, no vacuum of (a) cotton alone, (b) cotton + wine stain, (c) cotton + TiO_2 without pretreatment, (d) cotton + TiO_2 without pretreatment + wine stain and (e–g) cotton fabrics with TiO_2 pretreated for 10 min, no vacuum + wine stain.

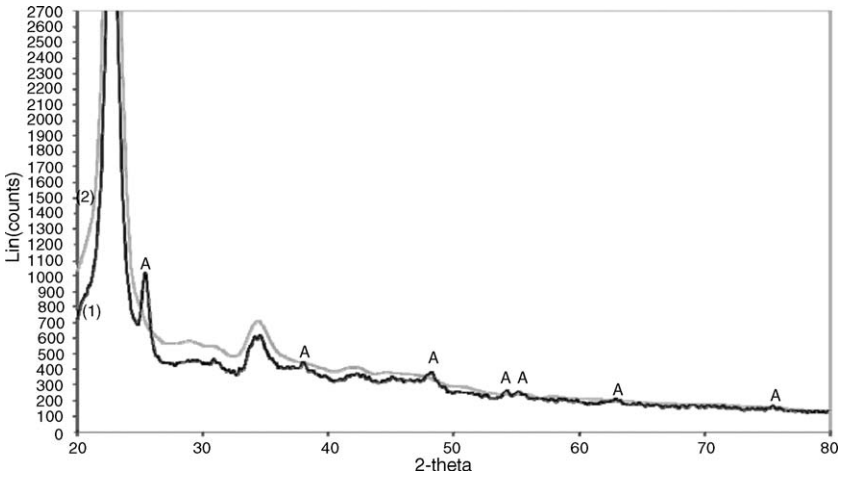

Fig. 9. X-ray diffraction patterns of (1) cotton fabric, (2) TiO_2-coated cotton pretreated by RF-plasma for 10 min, no vacuum (A, anatase).

amount of CO_2 (1739 μL) after 24 h of irradiation. Samples pretreated by RF-plasma for 10 min (sample 2) showed a CO_2 production of 1036 μL, however this quantity is very similar than that of the sample pretreated by RF at atmospheric pressure (trace h) during 30 min (1022 μL). TiO_2-coated cotton stained with red wine but without any pretreatment by RF is shown in trace (c), the amount of CO_2 produced during 24 h of irradiation was low (698 μL). Furthermore, very small amounts of CO_2 (55 μL) were observed when cotton was irradiated with daylight in the absence of TiO_2 and wine (trace a). Also, small amounts of CO_2 (91 μL) were found for cotton stained with wine in the absence of TiO_2 (trace b). These results show a similar trend for red wine discoloration on natural and synthetic TiO_2 textiles recently reported [31–33].

3.4.2. CO_2 evolution of cotton fabrics pretreated by UVC-light with and without vacuum

Fig. 7 presents the CO_2 evolution during the discoloration of wine stain for samples pretreated by UVC-light. Samples pretreated by vacuum-UV for 10 min (Fig. 7 trace J) showed the most favorable CO_2 evolution (1505 μL) after 24 h of irradiation. Nevertheless, this production is lower compared with that obtained by radio frequency (sample 2). Samples pretreated by vacuum-UV for 30 min (trace i) produce the second highest amount of CO_2 (1242 μL). Samples with 10 min of pretreatment by UVC-light at atmospheric pressure (trace h) produce 1081 μL of CO_2 after 24 h of irradiation. Although this amount is lower than that achieved by UVC, the absence of vacuum makes this pretreatment highly convenient for industrial textile application. Furthermore, the CO_2 released with sample (sample 11) is higher in μL CO_2 compared to the TiO_2-coated cotton stained with red wine but without any pretreatment (trace c). This suggests that the pretreatment of fabrics enhance the stain degradation. Only small amounts of CO_2 are observed in cotton irradiated with daylight in the absence of TiO_2 and wine (trace a) and in cotton fabrics stained with wine but in the absence of TiO_2 (trace b).

3.5. CO_2 mineralization reproducibility

To verify the CO_2 mineralization reproducibility of photoactive systems, three different samples of cotton were loaded with TiO_2 and pretreated by RF-plasma at atmospheric pressure (no vacuum) for 10 min. Later, samples were stained with the same quantity of red wine and irradiated during 24 h under Suntest light irradiation. CO_2 mineralization results for the three samples showed an experimental error of 2%, giving evidence for the reproducibility of the discoloration (Fig. 8).

3.6. XRD measurements of TiO_2-modified textiles

Fig. 9 shows the cotton textile and the TiO_2–cotton for a sample pretreated 10 min by RF-plasma, no vacuum showing the anatase peaks for the TiO_2 particles deposited on the cotton. The XRD spectra confirmed that TiO_2 anatase phase was deposited on the cotton (trace 1) [19,25]. This result is consistent with the XPS observation shown in Fig. 3. Also, peaks at 22.9° and 34.4° can be seen in both patterns (trace 1 and 2), which may be attributed to cotton.

3.7. HRTEM measurements of TiO_2-modified textiles

High-resolution transmission electron micrography of a TiO_2-coated sample pretreated by RF-plasma for 10 min, no vacuum at time zero is shown in Fig. 10. A fairly homogeneous coating is observed on the cotton surface. The average thickness of TiO_2 layer was found to be ∼31 nm (±10%) and was conserved after the 24 h

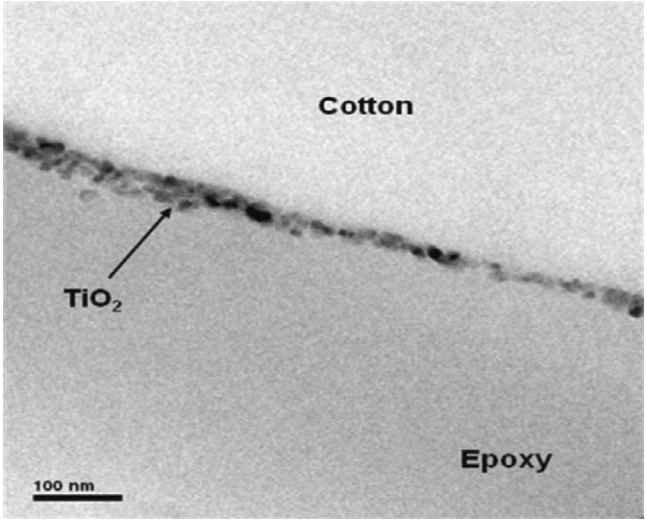

Fig. 10. TEM of TiO_2-coated cotton fabric at time zero, pretreated for 10 min, no vacuum.

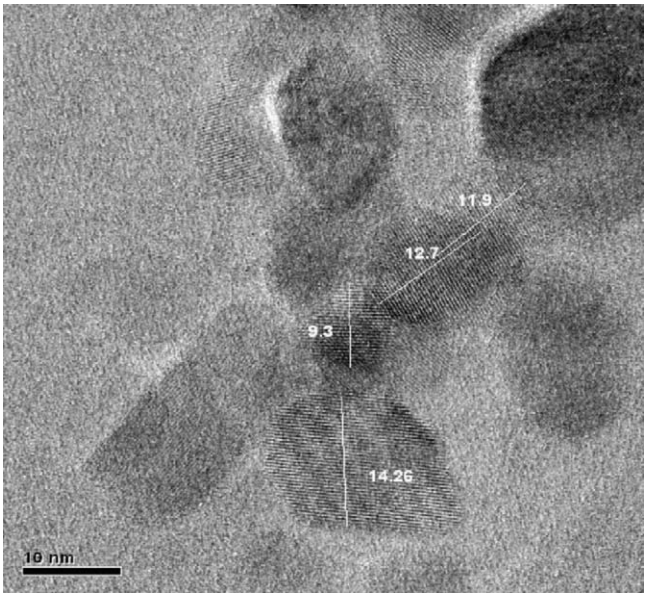

Fig. 11. HRTEM of TiO_2-coated cotton pretreated for 10 min, no vacuum showing the TiO_2 clusters and atomic planes (scale of 10 nm).

discoloration process. The TiO_2 particle size from about 8–18 nm is shown in Fig. 11, and was determined by high-resolution electron microscopy (HRTEM). This TiO_2 particle size was small enough to render transparent films and keep the original handling touch of the cotton. This feature is important for the potential application of TiO_2 cotton fabrics. Furthermore, these particles seem to have a large specific surface area useful in the photo catalysis. No atomic force microscopy (AFM) could be carried out on these samples due to rough and non-homogeneous nature of the cotton surface.

4. Conclusions

- Nanocrystalline anatine TiO_2 with small particles size distribution was successfully synthesized and subsequently loaded on cotton fabrics by two innovative non traditional approaches: (a) fabrics pretreated in air under RF-plasma at atmospheric pressure were able to bind TiO_2 due to the drastic localized heating of the cotton. This heat effect breaks the intermolecular H-bonding between the cellulose surface-OH groups of adjacent molecules and (b) by UVC-light (185 nm) pretreatment at atmospheric pressure lead to the formation of atomic O and excited O^* in the gas phase. This is possible due to the extremely low optical absorption of O_2 and N_2 at 185 nm.
- Good reproducibility for the discoloration was obtained in both cases for red wine stains under Suntest simulated solar light. High-resolution electron microscopy was used to determine the structure, particle size and of the 3 or 4 TiO_2 layers on the cotton surface. A more uniform coating of TiO_2 on cotton was obtained pretreating with UVC as compared to RF-plasma.
- Diverse complementary experimental techniques were used to characterize the TiO_2-modified cotton before and after photocatalytic discoloration.

Acknowledgements

The authors thank COLCIENCIAS and the University of Antioquia, Medellin and COST Action 540 PHONASUM ''Photocatalytic technologies and novel nanosurafce materials, critical issues'' Bern, for the financial support for this study.

References

[1] J.M. Herrmann, Top. Catal. 34 (1–4) (2005) 49–65.
[2] C. Karunakaran, R. Dhanalakshmi, Sol. Energy Mater. Sol. Cells 92 (2008) 588–593.
[3] N.A. Laoufi, D. Tassalit, F. Bentahar, Global Nest J. 10 (3) (2008) 404–418.
[4] S. Mozia, A.W. Morawski, M. Toyoda, M. Inagaki, Sep. Purif. Technol. 63 (2) (2008) 386–391.
[5] G. Zayani, L. Bousselmi, P. Pichat, F. Mhenni, A. Ghrabi, J. Environ. Sci. Health Part A Toxic/Hazard. Subst. Environ. Eng. 43 (2) (2008) 202–209.
[6] L. Petrov, V. Iliev, A. Eliyas, D. Tomova, G.L. Puma, J. Environ. Prot. Ecol. 8 (4) (2007) 881–909.
[7] R.A. Torres, J.I. Nieto, E. Combet, C. Petrier, C. Pulgarin, Appl. Catal. B 80 (1–2) (2008) 168–175.
[8] D. Gumy, S.A. Giraldo, J. Rengifo, C. Pulgarin, Appl. Catal. B 78 (1–2) (2008) 19–29.
[9] S. Brosillon, L. Lhomme, C. Vallet, A. Bouzaza, D. Wolbert, Appl. Catal. B 78 (3–4) (2008) 232–241.
[10] C. Maneerat, Y. Hayata, Trans. Asabe 51 (1) (2008) 163–168.
[11] A.S. Besov, A.V. Vorontsov, Catal. Commun. 9 (15) (2008) 2598–2600.
[12] J.M. Coronado, S. Suarez, R. Portela, B. Sanchez, J. Adv. Oxid. Technol. 11 (2) (2008) 362–369.
[13] J.M. Coronado, B. Sanchez, R. Portela, S. Suarez, J. Sol. Energy Eng. Trans. 130 (1) (2008) 115–120.
[14] G. Xiao, X. Wang, D. Li, X. Fu, J. Photochem. Photobiol. A 193 (2–3) (2008) 213–221.
[15] Th. Maggos, A. Plassais, J.G. Bartzis, Ch. Vasilakos, N. Moussiopoulos, L. Bonafous, Environ. Monit. Assess. 136 (1–3) (2008) 35–44.
[16] H. Yu, K. Zhang, C. Rossi, Indoor Built Environ. 16 (6) (2007) 529–537.
[17] T. Yuranova, V. Sarria, W. Jardim, J. Rengifo, C. Pulgarin, G. Trabesinger, J. Kiwi, J. Photochem. Photobiol. A 188 (2–3) (2007) 334–341.
[18] J. Medina-Valtierra, C. Frausto-Reyes, J. Ramirez-Ortiz, G. Camarillo-Martinez, Ind. Eng. Chem. Res. 48 (2) (2009) 598–606.
[19] W.S. Tung, W.A. Daoud, Acta Biomater. 5 (1) (2009) 50–56.
[20] J. Kasanen, M. Suvanto, T.T. Pakkanen, J. Appl. Polym. Sci. 111 (5) (2009) 2597–2606.
[21] A. Chabas, T. Lombardo, H. Cachier, M.H. Pertuisot, K. Oikonomou, R. Falcone, M. Verita, F. Geotti-Bianchini, Build. Environ. 43 (12) (2008) 2124–2131.
[22] F. Sayılkan, M. Asiltürk, N. Kiraz, E. Burunkaya, E. Arpaç, H. Sayılkan, J. Hazard. Mater. 162 (2–3) (2009) 1309–1316.
[23] L. Caballero, K.A. Whitehead, N.S. Allen, J. Verran, J. Photochem. Photobiol. A 202 (2–3) (2009) 92–98.
[24] J. Zhao, V. Krishna, B. Hua, B. Moudgil, B. Koopman, J. Photochem. Photobiol. A 94 (2) (2009) 96–100.
[25] C.J. Chung, C.C. Chiang, C.H. Chen, C.H. Hsiao, H.I. Lin, P.Y. Hsieh, J.L. He, Appl. Catal. B 85 (1–2) (2008) 103–108.
[26] F. Gordillo Delgado, K. Villa Gómez, C. Mejía Morales, Microelectron. J. 39 (11) (2008) 1333–1335.
[27] V. Nadtochenko, N. Denisov, O. Sarkisov, D. Gumy, C. Pulgarin, J. Kiwi, J. Photochem. Photobiol. A 181 (2006) 401–407.
[28] D. Gumy, C. Morais, P. Bowen, C. Pulgarin, S. Giraldo, R. Hajdu, J. Kiwi, Appl. Catal. B 63 (2006) 76–84.
[29] T. Yuranova, D. Laub, J. Kiwi, Catal. Today 122 (1–2) (2007) 109–117.
[30] K. Qi, J.H. Xin, W.A. Daoud, Int. J. Appl. Ceram. Technol. 4 (6) (2007) 554–563.
[31] A. Bozzi, T. Yuranova, J. Kiwi, J. Photochem. Photobiol. A 172 (2005) 27–34.
[32] A. Bozzi, T. Yuranova, I. Guasaquillo, D. Laub, J. Kiwi, J. Photochem. Photobiol. A 174 (2005) 156–164.
[33] K.T. Meilert, D. Laub, J. Kiwi, J. Mol. Catal A: Chem. 237 (2005) 101–108.
[34] Y. Dong, Z. Bai, R. Liu, T. Zhu, Atmos. Environ. 41 (15) (2007) 3182–3192.
[35] M.I. Mejía, J.M. Marín, Z. Díaz, L.A. Ríos, G. Restrepo, Rev. Colombiana de Física 39 (2) (2007) 559–562.
[36] M.I. Mejía, J.M. Marín, G. Restrepo, L.A. Ríos, Rev. Sci. Technol. 36 (2007) 97–102.
[37] Y. Ku, C.M. Ma, Y.S. Shen, Appl. Catal. B 34 (2001) 181–190.
[38] W. Kangwansupamonkon, V. Lauruengtana, S. Surassmo, U. Ruktanonchai, Nanomed.: Nanotechnol., Biol. Med. 5 (2009) 240–249.
[39] W.S. Tung, W.A. Daoud, J Colloid Interface Sci. 326 (2008) 283–288.
[40] M.J. Uddin, F. Cesano, D. Scarano, F. Bonino, G. Agostini, G. Spoto, S. Bordiga, A. Zecchina, J. Photochem. Photobiol. A 199 (2008) 64–72.
[41] Z. Liuxue, W. Xiulian, L. Peng, S. Zhixing, Surf. Coat. Technol. 201 (2007) 7607–7614.
[42] M.J. Uddin, F. Cesano, F. Bonino, S. Bordiga, G. Spoto, D. Scarano, A. Zecchina, J. Photochem. Photobiol. A 189 (2007) 286–294.
[43] T. Yuranova, R. Mosteo, J. Bandara, D. Laub, J. Kiwi, J. Mol. Catal. A 244 (2006) 160–167.
[44] G.A. Gaddy, M.S. Bratcher, G. Mills, S. Huang, B.L. Slaten, J. Debortoli, Proc. Army Sci. Conf., 24th, vol. 1, 100-114, 2005.
[45] Y. Dong, Z. Bai, R. Liu, T. Zhu, Catal. Today 126 (2007) 320–327.
[46] H. Wang, Z. Wu, W. Zhao, B. Guan, Chemosphere 66 (2007) 185–190.
[47] B.O. Bitlisli, A. Yumurtas, J. Soc. Leather Technol. Chem. 92 (5) (2008) 183–186.
[48] T. Yuranova, A.G. Rincon, C. Pulgarin, D. Laub, N. Xantopoulos, H.J. Mathieu, J. Kiwi, J. Photochem. Photobiol. A 181 (2006) 363–369.
[49] S. Frantz, G.A. Hüner, O. Wendland, E. Roduner, C. Mariani, M.F. Ottaviani, S.N. Batchelor, J. Phys. Chem. 109 (2005) 11572–11579.
[50] Cotton: World Markets and Trade; Circular FC 02-09; US Dept. Agriculture.
[51] C. Chan, T. Ko, H. Hiroaka, Surf. Sci. Rep. 24 (1996) 1–54.
[52] A. Johnson, The Theory of Coloration of Textiles, Society of Dyers and Colourists, England, 1989.

[53] S. Frantz, G.A. Hbner, O. Wendland, E. Roduner, C. Mariani, M.F. Ottaviani, S.N. Batchelor, J. Phys. Chem. B 109 (23) (2005) 11572–11579.
[54] Handbook of Chem. Phys., CRC Pub. Co., Boca Raton, FL, 2004.
[55] A. Shirley, A. Phys. Rev. A 179 (5) (1979) 4709–4716.
[56] M. Briggs, D. Shea, Practical Surface Analysis, 2nd Edition, v. 1 Auger and X-rays, Photoelectron Spectroscopy. John Wiley, Chicester, UK 1990.
[57] M.C. Hidalgo, M. Aguilar, M. Maicu, J.A. Navío, G. Colón, Catal. Today 129 (1–2) (2007) 50–58.
[58] J.A. Rengifo-Herrera, E. Mielczarski, J. Mielczarski, N.C. Castillo, J. Kiwi, C. Pulgarin, Appl. Catal. B: Environ. 84 (2008) 448–456.
[59] J. Bakker, C.F. Timberlake, J. Agric. Food Chem. 45 (1997) 35–43.